Atmos. Chem. Phys. Discuss., 12, 4341–4371, 2012
www.atmos-chem-phys-discuss.net/12/4341/2012/
doi:10.5194/acpd-12-4341-2012

Atmospheric Chemistry and Physics Discussions

AERONET and ESR sun direct products comparison performed on Cimel CE318 and Prede POM01 solar radiometers

V. Estellés[1,2], M. Campanelli[3], T. J. Smyth[4], M. P. Utrillas[1], and J. A. Martínez-Lozano[1]

[1]Dept. Física de la Terra i Termodinámica, Universitat de València, C/ Dr. Moliner 50, 46100 Burjassot, Spain
[2]Dept. Física Fundamental y Experimental, Electrónica y Sistemas, Universidad de La Laguna, Avda. Francisco Sánchez s/n, 38209 San Cristóbal de La Laguna, Santa Cruz de Tenerife, Spain
[3]Institute of Atmospheric Sciences and Climate, Italian National Research Council, Via Fosso del Cavaliere, Roma Tor Vergata, Italy
[4]Plymouth Marine Laboratory, Prospect Place, Plymouth PL1 3DH, UK

Received: 9 November 2011 – Accepted: 30 January 2012 – Published: 7 February 2012

Correspondence to: V. Estellés (victor.estelles@uv.es)

Published by Copernicus Publications on behalf of the European Geosciences Union.

Abstract

The *European Skynet Radiometers* network (EuroSkyRad or ESR) has been recently established as a research network of European Prede POM sun – sky radiometers. Moreover, ESR is federated with SKYNET (SKYrad NETwork), an international network mostly present in East Asia. In contrast to SKYNET, the European network also integrates users of the Cimel CE318 sunphotometer. Keeping instrumental duality in mind, a set of open source algorithms has been developed consisting of two modules for: (1) the retrieval of direct sun products from the sun extinction measurements; and (2) the inversion of the sky radiance to derive aerosol optical properties. In this study we evaluate the ESR direct sun products (spectral aerosol optical depth, Angström wavelength exponent and columnar content of water vapour) in comparison with the AERosol RObotic NETwork (AERONET) products. Specifically, we have applied the ESR algorithm to a Cimel CE318 and Prede POM01L simultaneously for a 4 yr database measured at the Burjassot site (Valencia, Spain), and compared the resultant products with the AERONET direct sun retrievals obtained with the same Cimel CE318 instrument. The comparison show that aerosol optical depth differences are mostly within the nominal uncertainty of 0.003 for a standard calibration instrument, and fall within the nominal AERONET uncertainty of 0.01–0.02 for a field instrument. Therefore, we present an open source code that can be used for both radiometers and whose results are comparable to those of AERONET and SKYNET.

1 Introduction

An accurate characterization of atmospheric aerosols is required to better quantify the Earth's radiative balance and hence address issues such as climate change. The aerosol radiative forcing uncertainty is larger ($-0.6 \pm 0.4\,\mathrm{W\,m^{-2}}$ for the direct effect) than the radiative forcing uncertainties due to greenhouse gases such as CO_2 ($1.8 \pm 0.2\,\mathrm{W\,m^{-2}}$) (IPCC, 2007). This uncertainty needs to be reduced to enable more accurate predictions on future climate states.

ACPD

12, 4341–4371, 2012

AERONET and ESR sun direct products comparison

V. Estellés et al.

To estimate the optical and radiative properties of aerosols in the atmosphere the sun – sky radiometric technique is the most accurate and widely used. This technique consists of measuring two main variables at ground level: direct irradiance from the sun, and diffuse radiance scattered from the sky. From the direct solar irradiance an estimate of the aerosol optical depth (AOD) can be determined; this parameter can be considered the most simple parameter describing the aerosol burden in the atmospheric column (Holben et al., 1998). Using a combination of the direct sun and diffuse sky radiation, inversion algorithms can be applied to obtain further optical and radiative aerosol properties, such as the aerosol single scattering albedo, scattering phase function, refractive index and size distribution.

For climate data records, the World Meteorological Organization (WMO) only recommends the use of sun – sky radiometric data from international networks with imposed standardization leading to data product traceability. Such networks must provide a traceable calibration procedure, reliable quality standards and homogeneity in the retrievals within the network.

An example for this is the NASA Aerosol Robotic Network (AERONET) (Holben et al., 1998), currently being the most extended operative network in the world. AERONET is mainly distributed in North America and Europe, and employs the Cimel CE318 sun photometer as the standard instrument. More than 250 Cimel units take part in the AERONET programme which adopts an original inversion algorithm to analyse the radiation components (Dubovik and King, 2000). However, the source code of this algorithm is not publicly available. This is important, as a good number of Cimel sites are not federated with AERONET. As the algorithm code is not available for these sites' managers, their data is not properly elaborated and the results are usually out the sight of the scientific community.

Another important international network is SKYrad NETwork (SKYNET) (Takamura and Nakajima, 2004). SKYNET is a research network mostly spread in Asia. Currently, it is composed of 37 sites and it holds the Prede POM radiometer as the standard instrument. The Prede data is processed using the Skyrad.pack (Nakajima et al., 1996)

ACPD
12, 4341–4371, 2012

code, currently at version 4.2 (Takamura and Nakajima, 2004). This code is open source code, and therefore it can be used by the site managers in order to colaborate on the improvement and validation of the procedures.

The European Skynet Radiometers network (EuroSkyRad or ESR) (ESR website, 2011) has been recently established as a network of European users of Cimel CE318 and Prede POM radiometers that focus their research on the atmospheric aerosols in Europe and the Mediterranean area. Currently, 12 sites take part in this network (Campanelli et al., 2012).

In contrast to both AERONET and SKYNET, the ESR does not hold any specific instrument as standard, but develops algorithms than can be applied to measurements from both instruments. In fact, one of the objectives of ESR is to perform synergistic studies with both networks and instruments. Keeping this instrument duality in mind, a new open source package (ESR.pack) has been developed. This package is partly based on the Skyrad.pack algorithm used in SKYNET, and has been modified, completed and adapted for application to Cimel radiometers as well.

The ESR.pack consists of two modules for: (1) the retrieval of direct sun products from the sun extinction measurements; and (2) the inversion of the sky radiance to derive further aerosol optical properties (phase function, single scattering albedo, complex refractive index and aerosol size distribution). In this study, we describe and validate the first module (called *sunrad*), intended for the estimation of aerosol optical depth, Angström wavelength exponent and columnar water vapour.

Two different versions or *modes* have been implemented in sunrad: mode 1 employs routines and assumptions extracted from the Skyrad.pack source code (version 4.2). The retrievals from mode 1 are therefore homogeneous with correspondent SKYNET products. In mode 2 we have implemented other routines that are much closer to those of AERONET direct sun algorithm (AERONET Website, 2011).

In this work we have addressed the validation of the two modes of the sunrad module by: (a) comparing the ESR (sunrad) and AERONET products using the same Cimel radiometer database; (b) studying the differences between Cimel and Prede radiometers products obtained using the same ESR processing algorithm; and (c) comparing the ESR-Prede products against AERONET-Cimel.

2 Instrumentation, calibration and methodology

2.1 Instrumentation

The CE318 sky – sun photometer is an automatic ground based radiometer measuring both direct solar irradiance and diffuse sky radiance for almucantar and principal solar planes with a 1.2° field of view limiting tube. The standard measuring schedule for this instrument broadly consists of direct sun triplets every 15 min, and sky diffuse almucantar or principal plane scenarios every 30 min. Although the channel wavelength configuration depends on the instrument version, filters at 440, 675, 870, 940 and 1020 nm wavelengths are always present.

A Cimel CE318 polar radiometer was installed in January 2002 at the Burjassot campus of the University of Valencia in Spain (39.51° N, 0.42° W, ∼30 m a.s.l.). During April 2007, the instrument started to operate within AERONET through the Red Ibérica de Medida de Aerosoles (RIMA) (RIMA website, 2011). This unit was serial number #422 and the filter wheel included channels at 440, 670, 870, 940 and 1020 nm. In February 2009, the optical head was upgraded to a UV version (filters at 340, 380, 440, 500, 675, 870, 940 and 1020 nm). From then on, other RIMA-AERONET units have substituted unit #422 in this site although the nominal channels remained the same. Therefore, data from instruments #422, #424 and #425 have been used in this study. The exact wavelengths are presented in Table 1.

The Prede POM-01L instrument is an automatic radiometer measuring direct sun and diffuse sky radiance with a 1.0° field of view columnator tube at 7 channels: 315, 443, 500, 675, 870, 940 and 1020 nm. The Prede POM design is broadly similar to Cimel sunphotometer, although it performs direct sun readings every minute and solar almucantar plane sky radiance every 10 or 20 min.

ACPD
12, 4341–4371, 2012

During January 2008, a Prede POM-01L radiometer was installed at the Burjassot site, allowing us to compare both Cimel and Prede retrievals. For this study, we have only used direct sun retrievals. The central wavelengths of the Prede filters are shown at Table 1. It must be taken into account that 340, 380 and 500 nm filters were not available for #422 Cimel before February 2009. Due to previous filter degradation, the 940 nm filter was also changed at the same time. The wavelength in the Table corresponds to the later filter. Moreover, standard POM instruments are equipped with a 400 nm filter, but the 440 nm filter was custom selected instead for a better match with the co-located Cimel sun-photometer.

2.2 Calibration

The Cimel photometers used in this study were calibrated by RIMA-AERONET. Pre- and post-calibrations were available for Cimel units #422 and #424. Only pre-calibration was available for unit #425. These calibrations are performed approximately on a yearly basis by a transfer from an AERONET master instrument (Holben et al., 1998). The nominal calibration uncertainty for field instruments can be estimated as 1–2 %, depending on channel. The resultant uncertainty of the aerosol optical depth for an AERONET field instrument was estimated to be about 0.01–0.02 (Eck et al., 1999) or about 10 % for a nominal aerosol optical depth of 0.1.

Generally, the calibration of Prede radiometers for the sun direct readings is obtained on site by the application of an improved in situ Langley technique (SKYIL method) (Campanelli et al., 2004a). Tests of the method on a Prede instrument in Rome showed a calibration accuracy of about 1.5–2.5 %, depending on the channel (Campanelli et al., 2004a). However, in order to exclude calibration effects in our study, the Prede calibration was transferred from the Cimel operating at the Burjassot site. These calibration transfers were periodically performed after May 2009. Therefore, for the comparison between Prede and Cimel, we have not used data before this date.

The calibration transfer consists of performing multiple and simultaneous direct sun measurements with two or more co-located instruments. In our case, the reference

ACPD
12, 4341–4371, 2012

(primary, or *master*) instrument was the Cimel, whose pre- and post- calibrations are provided by RIMA. The calibration for any given day used in the transfer process is linearly interpolated between these pre- and post-calibrations. On selected days, the master was set to measure only direct readings on a 1 min time resolution, matching the Prede (secondary instrument) minute measurements. Although a complete rotation of the filter wheel last different times for each radiometer (3 s in the case of Prede, 10 s in the case of Cimel), preliminary checks showed that a delay of a few seconds would not significantly affect the calibration transfer on stable days.

In order to reduce uncertainties introduced in the process, only cloudless and stable days were selected, and the measurements were usually performed around solar noon to avoid rapid changes in the air mass and optical depth that could lead to hidden trends in the coefficient ratios. A typical Prede transfer session consisted of the following: (a) a first leg of simultaneous one minute frequency measurements for approximately 1 h; (b) cleaning of the optical head windows, checking of the collimator, and adjustment of the solar pointing system; (c) a second leg of measurements lasting approximately 1 h. In this way, a post- and pre- calibration can be obtained from the first and second legs, respectively. These were then linearly interpolated to find a daily calibration for each day within the database.

If the instruments have a similar design and the differences in the central wavelengths are very small then, to a good approximation, we can obtain the secondary calibration by applying:

$$F_0^{\mathrm{s}}(\lambda_{\mathrm{s}}) = F_0^{\mathrm{p}}(\lambda_{\mathrm{p}}) \frac{F^{\mathrm{s}}(\lambda_{\mathrm{s}})}{F^{\mathrm{p}}(\lambda_{\mathrm{p}})} \quad (1)$$

where F and F_0 are the signal measured at ground and the extraterrestrial calibration respectively. In this equation, the subscripts refer to the primary (p) and secondary (s) instrument channels. In Table 1 the different filters were compared for all the instruments employed in this study. Most of the differences between Prede #046 and Cimel's are within 1–2 nm. The exceptions are at 440 nm and 940 nm, with a difference

ACPD
12, 4341–4371, 2012

of 5–6 nm in comparison to #424 and #425. In any case, these differences are smaller than the bandwidths (nominally 10 nm at the visible and near infrared range).

An example of the calibration transfer is presented in Fig. 1, performed on 11 May 2011. In this calibration session the procedure described above was followed as closely as possible. In the figure, the two legs of instantaneous calibration coefficients obtained through the use of Eq. (1) are represented. The first leg leads to the *post-calibration*, that is, the calibration obtained after a field data series is completed. The second leg leads to the so called *pre-calibration*, that is, the calibration prior to the next field data series to be started. The jump between the two calibration legs are due to the cleaning of optical head windows and adjustment of the pointing system. The root mean square deviation of the series was estimated to be 0.12–0.23 % depending on channel: this was a maximum for 940 nm and a minimum for 870 nm channels.

2.3 Implementation of the *sunrad* module

The ESR.pack is composed of two different modules: (a) *sunrad*, for deriving aerosol optical depth, Angström exponent and columnar water vapour from the direct sun readings; and (b) *skyrad*, a modified version of the Skyrad.pack (Nakajima et al., 1996; Kobayashi et al., 2010) version 4.2, to invert the sky radiance measurements and obtain further aerosol properties such as size distribution, phase function, single scattering albedo and complex refractive index. In this section we will present the new sunrad.pack module and the algorithms implemented within it. The software is programmed in open source FORTRAN. Deliverable versions of sunrad and skyrad programs will be made public through the ESR website (2011).

Mirroring the structure of the Skyrad.pack software, the sunrad module has been implemented in two separate parts: a formatting program (*dsform*) reads the Cimel and Prede data files and converts them to a common data format file; then, a processing program (*dsproc*) reads the formatted data files and retrieves the AOD and other columnar variables.

ACPD
12, 4341–4371, 2012

Both dsform and dsproc programs have been implemented in two different versions or *modes*: mode 1 mostly includes pre-existing subroutines from the Skyrad version 4.2, extracted from the source code. Therefore, this mode is identical to the SKYNET methodology. Mode 2 includes new algorithms to derive the solar coordinates, optical mass, absorption coefficients and gaseous optical depths. These algorithms are very similar to those implemented in version 2 of the AERONET sun direct algorithm (AERONET Website, 2011). Therefore, our results should be the same as the Cimel AERONET measurements.

In Table 2 the differences between the mode 1 and 2 algorithms are listed. Mode 1 uses a single optical mass calculated for a parallel atmosphere, older algorithms for the estimation of the Rayleigh scattering, and do not consider the effect of water vapour and NO_2 absorption. Mode 1 also includes the convolution of gaseous absorption spectra by Gaussian transmission profiles calculated from the central nominal or exact wavelengths, and associated FWHM given in the configuration file. The Angström exponent is computed from the ratio of AOD at two different wavelengths, for UV, VIS and NIR ranges.

The mode 2 algorithm data set is based in the previous work of Estellés et al. (2006, 2007) and includes the following subroutines: a more accurate solar position algorithm (Blanco-Muriel et al., 2001) with a refraction correction of the solar zenith angle (Michalsky et al., 1988); an optical mass based on (Kasten et al., 1989), different for ozone calculation (Komhyr et al., 1989) and the computation of optical depths removing the effects of water vapor and NO_2. The Angström exponents are obtained by a linear fitting in the ranges UV, VIS and NIR for a more robust estimation (Martínez-Lozano et al., 1998). Moreover, the real transmission profiles of the filters can be used to convolute the absorption coefficient spectra from all three gases and CO_2.

For the retrieval of the columnar water vapour (CWV) the Bruegge et al. (1992) methodology with the generic coefficients proposed by Halthore et al. (1997) has been implemented. This methodology was actually employed in previous versions of AERONET direct sun algorithm version 1. Future developments of the ESR codes will include improved methodologies to derive the precipitable water content in mode 2, consistent with the AERONET version 2 methodology (AERONET Website, 2011). For mode 1, the method developed by Campanelli et al. (2010) will be used, consistent with SKYNET.

In order to quality assure the data and avoid cloud contamination, the basic Smirnov et al. (2001) cloud screening algorithm was also implemented in both modes. This is based on a set of criteria controlling the temporal variability of the AOD. This cloud screening method was designed for its use on Cimel data, making use of the standard direct sun triplets used by this instrument. Therefore, its application to the Cimel is straightforward. However, the Prede radiometer must be configured to perform sun measurements every minute. Equivalent triplets can be built during the data formatting stage, so equivalent triplet criteria are imposed.

Another important issue when comparing Cimel and Prede instruments is the temperature effect on the Silicon photo-diode readings, whose effect is described by Eq. (2). In this equation, F_{25} refers to the corrected reading at a temperature of 25 °C, and F_T refer to the reading at a temperature T. The thermal coefficient is $k_T(\lambda)$, expressed in %/°C. These coefficients depend on wavelength (λ) and can be estimated by experiments with a stabilized source lamp on a dark thermal chamber (Taviro, 2011). Our experiments for Cimel #422 showed thermal coefficients only slightly different to those published by Holben et al. (1998).

$$F_{25}(\lambda) = F_T(\lambda)[1 + \frac{k_T(\lambda)}{100}(T - 25)]^{-1} \quad (2)$$

Different methodologies to account for the temperature effect are used on both instruments. The Cimel cannot control the sensor temperature, but it is routinely measured and can be corrected afterwards. In contrast, standard Prede radiometers do not measure the sensor temperature, but the sensor is temperature stabilised. In the sunrad module, a subroutine for temperature correction is included. Generic thermal coefficients can be used for the most sensitive channels from Cimel (1020 nm and 870 nm) (Holben et al., 1998), but instrument specific coefficients can be fed also, if available.

ACPD
12, 4341–4371, 2012

Obviously, the correction is only applied when the sensor temperature is available. This was not the case for our Prede radiometer.

2.4 Comparison methodology

To perform the validation of the sunrad module (modes 1 and 2) and AERONET direct sun algorithm version 2, the Cimel database obtained at Burjassot site (Valencia, Spain) has been used. More specifically, the study is limited to a subset spanning from April 2007 to June 2011 (for Cimel) and May 2009 to June 2011 (for Prede).

The pre- and post-calibrations for the Cimel's were provided by RIMA/AERONET for units #422 (April 2007 to October 2009) and #424 (October 2009 to February 2011). Only pre-calibration is available for #425. As for AERONET, in the sunrad module the calibration for any given day is obtained by linear interpolation between pre- and post-calibration, and corrected by the Sun-Earth distance to get the effective calibration factor.

Ozone columnar burden has been obtained from the OMI sensor and correspondingly interpolated for any instantaneous measurement (OMI website, 2011). NO_2 and water vapor were not available at this site, so they have been selected from published climatological values and standard atmospheres (Gueymard, 2001).

To estimate the gaseous absorption coefficients, we have employed the filter transmission profiles provided by the Cimel and Prede companies for our instruments (Cimel #422 and Prede #046). RIMA also provided new filters for #422 and other network instruments (#424 and #425). In mode 2, the real profiles were actually supplied in an input file and the absorption coefficients convoluted with them in the dsform program.

Level 2.0 products for #422 Cimel were downloaded from the AERONET website (except AOD at 340 nm, that only attains level 1.5). Only level 1.5 products were available for #424 and #425. Although level 1.5 data would be not appropriate for a climate data record, it is perfectly valid for comparison purposes. The evolution of AERONET AOD at 440 nm is shown in Fig. 2. The AOD seasonal evolution was in agreement with a previous 4 yr climatology performed at this site (Estellés et al., 2007), with higher

Discussion Paper | Discussion Paper | Discussion Paper | Discussion Paper |
ACPD
12, 4341–4371, 2012

AOD during the summertime, and low values during the wintertime. The mean AOD at 440 nm during the data bench period was 0.18 ± 0.11, and the values vary from a background value of 0.08 (25th percentile) to occasional episodes overpassing 0.38 (95th percentile).

To estimate the deviation between sunrad module products and AERONET, different statistical indicators have been calculated: root mean square deviation (rmsd), mean bias deviation (mbd) and the standard deviation of differences (std). Equations (3) to (5) show these estimators. U95 and the rmsd expressed as a percentage were also computed. The Chauvenet criterion has been applied to avoid outliers in the sample, by removing any point with a difference from the mean greater than 3 times the sample standard deviation. In the following expressions, δ_{0i} and δ_i refer to the AOD from the reference and secondary instruments, respectively, and Δ_i represents the difference between two simultaneous δ_{0i} and δ_i.

$$\mathrm{RMSD} = \sqrt{\frac{1}{N}\sum_{i=1}^{N}(\delta_{0i}-\delta_i)^2} = \sqrt{\frac{1}{N}\sum_{i=1}^{N}\Delta_i^2} \tag{3}$$

$$\mathrm{MBD} = \overline{\Delta} = \frac{1}{N}\sum_{i=1}^{N}(\delta_{0i}-\delta_i) = \frac{1}{N}\sum_{i=1}^{N}\Delta_i \tag{4}$$

$$\mathrm{STD} = \sqrt{\frac{1}{N}\sum_{i=1}^{N}(\Delta_i-\overline{\Delta})^2} \tag{5}$$

Finally, the comparison between Prede-ESR and the Cimel-ESR or Cimel-AERONET products have also been computed for all the coincident channels (including 440 nm and 443 nm pair, despite its larger wavelength displacement), using the same equations given above. Moreover, two Prede and Cimel retrievals are considered coincident when the time difference between their acquisitions is less than 30 s.

3 Results

3.1 Comparison of ESR and AERONET for Cimel photometer

The performance of sunrad when applied to the same Cimel photometer analysed by AERONET has been assessed in this section. The same calibration factors and dataset have been used, so the differences between both products should be a minimum. In Fig. 3, the differences (daily averaged) between ESR and AERONET for AOD675, AOD1020, Angström exponent (AE) and CWV retrievals, for mode 1 are shown. The statistics are presented in Table 3 (top table). In general, the AOD retrieved by sunrad (mode 1) is comparable with AERONET, getting mbd values between −0.0030 and 0.0041 (0.012 in the case of AOD340). The AOD differences are usually highest at 340 nm, due to the higher signal to noise ratio in the UV region and uncertainties related to the estimation of the ozone optical depth. Moreover, the mbd signs show that the AOD is slightly underestimated by the sunrad (mode 1) algorithm, except for the 1020 channel.

The quadratic deviations (given by the rmsd) are higher, ranging from 0.0084 to 0.013 (0.018 in the case of AOD340). This increase in comparison to the mbd is related to a seasonal variability, produced by inaccuracies of the solar position and optical mass routines implemented in the sunrad mode 1. This effect is strongly apparent in the temporal evolution of the differences, shown in Fig. 3. These rms deviations are still below the AERONET estimated uncertainty for a field instrument (0.01–0.02 uncertainty depending on channel, higher at shorter wavelengths). The 340 and 440 nm channels are the exception, with an u95 percentile occasionally reaching or even surpassing this nominal uncertainty. Represented as a percentage, the AOD deviations vary between 5 to 11 %.

For AE and CWV, the rmsd is 0.12 and 0.17 cm respectively. The CWV uncertainty is related to the propagation of errors from AE, the simplistic air mass calculation, and the lack of water vapor corrections in AOD1020 for mode 1.

ACPD
12, 4341–4371, 2012

If switched to mode 2, the results improve at all channels, especially for 340, 440 and 870 nm. Figure 4 show the evolution of the differences. The improvement can also be detected in the u95 percentiles. The mbd is insignificant, ranging from −0.0021 to +0.0007. In this case, the sunrad algorithm under- or overestimates depending on the channel. The rms deviation ranges between only 0.0005–0.0018, with the highest deviation in the UV channels (0.0051 for AOD340). For the VIS-NIR region, channel 1020 nm has the largest deviation (0.0019). This relative deviation could be related to uncorrected differences in the thermal constants or residual effects of the water vapor correction. In contrast to mode 1, the standard deviation of the differences (std) is also very low (0.0002 to 0.0030, only 0.0050 in the case of AOD340) showing that the mean deviations are representative of the whole sample. In fact, the seasonal variability has completely disappeared, as can be seen in Fig. 4. On a percentage scale, the AOD deviation is found to be between 0.5 and 2.0 %.

The results are also better than mode 1 for AE and CWV parameters. For AE, the mbd and rms deviations are −0.007 and 0.017, respectively. The lower AOD and AE differences led to a mbd and rmsd of −0.008 and 0.15 cm, respectively. Residual differences could be still decreased by changing the water vapor algorithm to the current version used in AERONET, using also individual constants for each 940 nm filter. In our case, only generic constants are assumed, based on the values given by Halthore et al. (1997).

3.2 Comparison of ESR for Cimel and Prede radiometers

Table 4 shows a statistical comparison between Cimel and Prede retrievals, obtained with the same sunrad code and identical input parameters (ozone, atmospheric pressure), for modes 1 and 2. No results are available for 340 and 380 nm channels, because of different filter configurations between the instruments (Table 1). The database for this comparison is limited to Prede and Cimel matching years of 2009–2011.

The results presented in Table 4 show that equivalent AOD, AE and CWV retrievals are obtained with Cimel and Prede radiometers for both modes 1 and 2. For AOD, the

ACPD
12, 4341–4371, 2012

mbd ranges between −0.0023 to +0.0044 in both modes, and the rmsd varies between 0.0022 and 0.0057.

Maximum deviations are obtained for channels 1020 nm (probably due to residual temperature effects) and 500 nm. The difference in 500 nm channel is maximum when using mode 2, due to the use of the exact filter transmission profiles, that are used on turn to obtain the effective absorption coefficients of gases. It must be noted that the AOD is very sensitive to the effective absorption coefficients in some channels, dependent on the exact filter transmission shape (Kocifaj and Gueymard, 2011). Therefore the methodology to obtain these coefficients has an impact on the final AOD obtained. In any case, the differences are always within the estimated uncertainties.

The differences between both instruments are almost identical for both modes, and are slightly higher than the differences found in the previous section due to the increase of uncertainty on the calibration transfer to the Prede, and the differences on the exact filter transmission profiles.

For AE and CWV, the differences are also very low and independent of the mode, with an average rmsd of 0.006 and 0.05 cm, respectively. In the case of CWV, the deviation is lower than the deviation obtained in the previous section. The 0.05 cm value would be a measure of the ability of the sunrad code to obtain water vapour columnar amounts from the Prede instrument, in comparison to Cimel. This is a very useful result, as the Prede radiometers are not currently used for the retrieval of this important atmospheric variable.

New algorithms for the retrieval of CWV have been proposed during the past few years (Mavromatakis et al., 2007; Campanelli et al., 2012). The Mavromatakis et al. (2007) method proposes an improvement to the Bruegge et al. (1992) method for Cimel instruments, and is expected to be implemented on the sunrad code for mode 2. The Campanelli et al. (2010) algorithm was proposed for its use on the SKYNET Prede radiometers and currently is undergoing validation. This methodology will be implemented for mode 1 allowing for an accurate comparison between retrieval algorithms and instruments.

ACPD
12, 4341–4371, 2012

3.3 Comparison of ESR-Prede and AERONET-Cimel

Table 5 shows a statistical comparison between ESR-Prede and AERONET-Cimel retrieved aerosol optical depths. The statistics have been estimated over 550 days distributed over 3 yr for the period 2009–2011. No 340 and 380 nm channels are available for the comparison, due to differences in the Prede and Cimel filter configuration.

Overall, Table 5 shows an acceptable agreement for mode 1 and a quite good agreement for mode 2. The mbd for mode 1 spans from −0.0004 to +0.0057, although the corresponding rms deviation is between 0.0085 and 0.0117. The highest deviation corresponds to the 1020 nm filter. With a rms deviation of 0.15 and 0.20 cm, AE and CWV deviations are comparable to previous Sect. 3.1.

Furthermore, mode 2 performs much better in comparison to AERONET. When mode 2 is switched on, the rms deviation is kept low for AOD (0.0027–0.0054 for all channels) and AE (0.057). Even the u95 percentiles are maintained below this nominal uncertainty. On the contrary, the columnar water vapour reaches the limit of its estimated uncertainty (0.20 cm).

4 Discussion

Only a few published Cimel-Prede studies are available for comparison with our results and all of them were performed by the application of different code to each instrument, usually for very short periods and with different ways of reporting the quantitative deviations.

Sano et al. (2003) reported a single day of intercomparison of Cimel-AERONET and Prede-SKYNET aerosol optical depths, with a deviation between both datasets of less than 0.008 at 670 nm. Despite only a single day being presented, this value is very similar to ours for this channel when using mode 1 (rmsd of 0.0089) but higher than ESR on mode 2 (rmsd of 0.0027). No quantitative comparisons were provided for the other channels.

Campanelli et al. (2004b) performed a more detailed intercomparison between a Cimel-AERONET and a co-located Prede dataset using the Skyrad 4.2 inversion algorithm (mostly equivalent to ESR at mode 1) for a two week period in Rome, Italy. The deviations expressed as percentage were 10–12 %, for a mean AOD at 500 nm of about 0.12. The equivalent percentage rms deviation obtained by this work for the two year Cimel-AERONET and Prede-ESR comparison has been 5.5–14 % in the equivalent mode 1. Mode 2 improved the difference to 2.1–5.7 %.

Evgenieva et al. (2008) presented an intercomparison exercise between a Cimel-AERONET and Prede-SKYNET at Belsk (Poland) over a period of two days. The lowest deviation was found at 675 nm channel, with a AOD relative difference of about 8 %. The corresponding deviation was found by us to be 8.0 % in mode 1.

In a more extensive study, Che et al. (2008) stated the need to perform more extended intercomparisons between these instruments in order to better address the differences between networks in Asia. This study was conducted in Beijing (China). For the direct sun readings, a total of 3169 instantaneous measurements retrieved during 220 days were used. In this case the deviation was reported as the relative difference of the mean aerosol optical depth for both databases, resulting in 0.91 % at 440 nm, 1.03 % at 670 nm, 1.27 % at 870 nm and 0.82 % at 1020 nm.

Che et al. (2008) values are significantly lower than ours, whether we use mode 1 (5–14 %) or mode 2 (2–6 %). However, Beijing is characterized by frequent strong haze and dust dominated situations, with very high and extreme aerosol burdens (AOD at 440 nm frequently reaches extreme values such as 3.0). Therefore, the relative differences must be significantly reduced in comparison with our case, with a mean AOD at 440 nm of about 0.18 ± 0.11 and a percentile u95 of 0.38 (one order of magnitude lower than Beijing events). Unfortunately, the rmsd in absolute values were not reported in their work.

In general, the mode 1 (SKYNET equivalent) Prede-ESR against Cimel-AERONET intercomparisons are equivalent to previously published values; we have considerably improved on the temporal and spectral representativity. Mode 2 has further improved

ACPD
12, 4341–4371, 2012

on the mode 1 comparison, leading to retrievals much closer to AERONET values.

5 Conclusions

In order to produce a valid climate data record, it is critical to use standardized and traceable data sources. AERONET is an operational international network devoted to the retrieval of accurate aerosol properties, with a strong emphasis put on the traceability and homogeneity of the data. However, the algorithms used by AERONET are not freely available and therefore, independent investigators cannot easily participate in the further development and validation of the algorithms.

Other international research networks have developed similar algorithms using open source code, such as SKYNET. However, SKYNET algorithms are adapted to a different radiometer, and therefore, can not be directly used with Cimel instruments. To retrieve comparable aerosol properties, it is mandatory to use equivalent procedures for both instruments.

To overcome this difficulty, the European Skynet Radiometers network (ESR) has implemented a new algorithm package (called ESR.pack) that can be used in both AERONET and SKYNET standard instruments. In order to provide direct sun products equivalent to AERONET and SKYNET retrievals, two versions or *modes* have been implemented, and their results have been compared with AERONET.

Eventually, the ESR package will eventually be applied to all the Prede POM and Cimel CE318 radiometers from the Euroskyrad network. The objective of the network is to serve as a research platform where new techniques can be developed and validated, at the same time that independent instruments benefit of a higher degree of homogeneity within the ESR network and in comparison to other networks.

In this study, we have assessed the performance of the sunrad module in comparison to AERONET products. A 4 yr database (2007–2011) of Cimel measurements performed at the Burjassot site in Valencia (Spain) has been used for this purpose. The assessment performed with the Cimel data shows that both sunrad modes can

ACPD
12, 4341–4371, 2012

correctly reproduce the AERONET retrievals well within the related uncertainties (maximum rmsd of 0.013) although mode 2 offers much lower differences than mode 1, as expected (maximum rmsd of 0.0036). For water vapor, the rmsd was 0.17 cm and 0.15 cm for modes 1 and 2, respectively.

The performance of sunrad code to obtain comparable products from both Cimel CE318 and Prede POM01L has also been studied. The differences when using both modes are also low, with a rmsd of 0.0022–0.0057, independent of the mode.

Finally, Prede-ESR and AERONET AOD differ by a rmsd less than 0.012 and 0.0054 for modes 1 and 2 respectively, these results being obviously dependent on the homogeneity of the calibrations used in the radiometers.

Acknowledgements. The authors acknowledge RIMA and AERONET for providing retrievals and CE318 calibration coefficients. We also thank K. Inei from Prede Co. for his valuable advice on POM technical issues. V. Estellés thanks the Spanish Ministry of Science and Innovation (MICINN) for the research contract under the *Juan de la Cierva* programme (JCI-2009-04455). The Solar Radiation Group at the University of Valencia has been supported by projects CGL2011-24290 and CGL2009-07790 from the MICINN, and PROMETEO/2010/064 from the Valencia Autonomous Government. T. J. Smyth was supported by NERC ADIENT (NE/E011144/1).

References

AERONET website, http://aeronet.gsfc.nasa.gov, 2011. 4344, 4349, 4350

Blanco-Muriel, M., Alarcón-Padilla, D. C., López-Moratalla, T., and Lara-Coira, M.: Computing the solar vector, Solar Energy, 70, 431–441, 2001. 4349, 4364

Bodhaine, B. A., Wood, N. B., Dutton, E. G. and Slusser, J. R.: On Rayleigh optical depth calculations, J. Atmos. and Ocean Tech., 16, 1854–1861, 1999. 4364

Bruegge, C. J., Conel, J. E., Green, R. O., Margolis, J. S., Holm, R. G., and Toon, G.: Water Vapor Column Abundance Retrievals During FIFE, J. Geophys. Res., 97, 18759–18768, 1992. 4349, 4355, 4364

Red Ibérica de Medida de Aerosoles, http://www.rima.uva.es, 2011. 4345

Campanelli, M., Nakajima, T., and Olivieri, B.: Determination of the Solar Calibration Constant for a Sun-Sky Radiometer: Proposal of an In-Situ Procedure, Appl. Optics, 43, 651–659, 2004. 4346

Campanelli, M., Gobbi, G., Tomasi, C., and Nakajima, T.: Intercomparison between aerosol characteristics retrieved simultaneously with a Cimel and Prede sun-sky radiometers in Rome (Tor Vergata AERONET site), Óptica Pura y Aplicada, 37, 3159–3164, 2004. 4356

Campanelli, M., Lupi, A., Nakajima, T., Malvestuto, V., Tomasi, C., and Estellés V.: Summertime columnar content of atmospheric water vapor from ground based Sun sky radiometer measurements through a new in situ procedure, J. Geophys. Res., 115, D19304, doi:10.1029/2009JD013211, 2010. 4350, 4355

Campanelli, M., Estelles, V., Smyth, T., Tomasi, C., Martnez-Lozano, J. A., Claxton, B., Muller, P., Pappalardo, G., Pietruczuk, A., Shanklin, J., Colwell, S., Wrench, C., Lupi, A., Mazzola, M., Lanconelli, C., Vitale, V., Congeduti, F., Dionisi, D., Cardillo, F., Cacciani, M., Casasanta, G. P., and Nakajima, T.: Monitoring of Eyjafjallajoekull volcanic aerosol by the new European SkyRad users (ESR) sun-sky radiometer network, Atmos. Environ., 48, 33–45, doi:10.1016/j.atmosenv.2011.09.070, 2012. 4344, 4355

Che, H., Shi, G., Uchiyama, A., Yamazaki, A., Chen, H., Goloub, P., and Zhang, X.: Intercomparison between aerosol optical properties by a PREDE skyradiometer and CIMEL sunphotometer over Beijing, China, Atmos. Chem. Phys., 8, 3199–3214, doi:10.5194/acp-8-3199-2008, 2008. 4357

Eck, T., Holben, B. N., Reid, J. S., Dubovik, O., Smirnov, A., O'Neill, N. T., Slutsker, I., and Kinne, S.: Wavelength dependence of the optical depth of biomass burning urban and desert dust aerosols, J. Geophys. Res., 104, 31333–31349, 1999. 4346

Estellés, V., Utrillas, M. P., Martínez-Lozano, J. A., Alcántara, A., Olmo, F. J., Alados-Arboledas, L., Lorente, J., Cachorro, V., Horvath, H., Labajo, L., de la Morena, B., Vilaplana, J. M., Díaz, A. M., Díaz, J. P., Elias, T., Silva, A. M., Pujadas, M., and Rodríguez, J. A.: Aerosol related parameters intercomparison of Cimel sunphotometers in the frame of the VELETA 2002 field campaign, Óptica Pura y Aplicada, 37, 3289–3297, 2004.

Estellés, V., Utrillas, M. P., Martínez–Lozano, J. A., Alcántara, A., Alados-Arboledas, L., Olmos, F. J., Lorente, J., De Cabo, X., Cachorro, V., Horvath, H., Labajo, A., De La Morena, B., Díaz, J. P., Díaz, A. M., Silva, Elías, T., Pujadas, M., Rodriguez, J. A., Cañada, J., and García, Y.: Intercomparison of spectroradiometers and sunphotometers for the determination of the aerosol optical depth during the VELETA2002 field campaign, J. Geophys. Res., 111,

D17207, doi:10.1029/2005JD006047, 2006. 4349
Estellés, V., Martínez–Lozano, J. A., Utrillas, M. P., and Campanelli, M.: Columnar aerosol properties in Valencia (Spain) by ground-based Sun photometry, J. Geophys. Res., 112, D11201, doi:10.1029/2006JD008167, 2007. 4349, 4351
ESR website, http://www.euroskyrad.net, 2011. 4344, 4348
Evgenieva, T., Iliev, I., Koleva, N., Sobolewski, P., Pieterczuk, A., Holben, B. N., and Kolev, I.: Optical characteristics of aerosol determined by Cimel, Prede, and Microtops II sun photometers over Belsk (Poland), Proc. SPIE, 7027, doi:10.1117/12.822507, 2008. 4357
Dubovik, O. and King, M. D.: A flexible inversion algorithm for retrieval of aerosol optical properties from sun and sky radiance measurements, J. Geophys. Res., 105, 20673–20696, 2000. 4343
Fröhlich, C. and Shaw, G. E.: New determination of Rayleigh scattering in the terrestrial atmosphere, Appl. Optics, 19, 1773–1775, 1980. 4364
Gueymard, C. A.: Parameterized transmittance model for direct beam and circumsolar spectral irradiance, Solar Energy, 71, 325–346, 2001. 4351, 4364
Halthore, R. N., Eck, T. F., Holben, B. N., and Markham, B. L.: Sun photometric measurements of atmospheric water vapor column abundance in the 940 nm band, J. Geophys. Res., 102, 4343–4352, 1997. 4349, 4354, 4364
Holben, B. N., Eck, T. F., Holben, B. N., Slutsker, I., Buis, J. P., Setzer, A., Vermote, E., Reagan, J. A., Kaufman, Y., Nakajima, T., Lavenu, F., and Smirnov, A.: AERONET – A federated instrument network and data archive for aerosol characterization, Remote Sens. Environ., 66, 1–16, 1998. 4343, 4346, 4350
Kasten, F. and Young, A. T.: Revised optical air mass tables and approximation formula, Appl. Opt., 28, 4735–4738, 1989. 4349, 4364
Kobayashi, E., Uchiyama, A., Yamazaki, A., and Kudo, R.: Retrieval of Aerosol Optical Properties Based on the Spheroid Model, J. Meteorol. Soc. Japan, 88, 847–856, 2010. 4348
Komhyr, I. D., Grass, K. D., and Leonar, R. K.: Dobson spectrophotometer 83: a standard for total ozone measurements 1962–1987, J. Geophys. Res., 94, 9847–9861, 1989. 4349, 4364
Kocifaj, M. and Gueymard, C. A.: Theoretical evaluation of errors in aerosol optical depth retrievals from ground-based direct-sun measurements due to circumsolar and related effects, Atmos. Environ., 45, 1050–1058, 2011. 4355
Intergovernmental Panel on Climate Change (IPCC), edited by: Solomon, S., Qin, D., Manning, M., Chen, Z., Marquis, M., Averyt, K. B., Tignor, M., and Miller, H. L., Climate Change 2007:

ACPD
12, 4341–4371, 2012

AERONET and ESR sun direct products comparison

V. Estellés et al.

The Physical Science Basis. Contribution of Working Group I to the Fourth Assessment Report of the Intergovernmental Panel on Climate, 2007. 4342

Martínez-Lozano, J. A., Utrillas, M. P., Tena, F., and Cachorro, V.: The parameterisation of the atmospheric aerosol optical depth using the Angström power law, Solar Energy, 63, 303–311, 2007. 4349

Mavromatakis, F., Gueymard, C. A., and Franghiadakis, Y.: Technical Note: Improved total atmospheric water vapour amount determination from near-infrared filter measurements with sun photometers, Atmos. Chem. Phys., 7, 4613–4623, doi:10.5194/acp-7-4613-2007, 2007. 4355

Michalsky, J. J.: The astronomical almanac's algorithm for approximate solar position (1950–2050), Solar Energy, 40, 227–235, 1988. 4349, 4364

Nakajima, T., Tonna, G., Rao, R., Boi, P., Kaufman, Y., and Holben, B.: Use of sky brightness measurements from ground for remote sensing of particulate polydispersions, App. Opt., 35, 2672–2686, 1996. 4343, 4348

Ozone Monitoring Instrument website, http://ozoneaq.gsfc.nasa.gov, 2011. 4351

Sano, I., Mukai, S., Yamano, M., Takamura, T., Nakajima, T., and Holben, B.: Calibration and validation of retrieved aerosol properties based on AERONET and SKYNET, Adv. Space Res., 32, 2159–2164, 2003. 4356

Smirnov, A., Holben, B. N., Eck, T. F., Dubovik, O., and Slutsker, I.: Cloud screening and quality control algorithms for the AERONET database, Remote Sens. Environ., 73, 337–349, 2000. 4350, 4364

Takamura, T. and Nakajima, T.: Óptica Pura y Aplicada, 37, 3303–3303, 2004. 4343, 4344

Taviro, F.: Determination of the thermal coefficient from Cimel CE318 sunphotometers, Degree project (in Spanish), Universitat de València, Burjassot, 46 pp., 2011. 4350

Young, A. T.: On the Rayleigh scattering optical depth of atmosphere, J. Appl. Meteorol., 20, 328–330, 1981. 4364

ACPD

12, 4341–4371, 2012

AERONET and ESR sun direct products comparison

V. Estellés et al.

Table 1. Filter wavelengths corresponding to central maximum for the employed Cimel (#422, #424 and #425) and Prede radiometers (#046).

Ch.	$\lambda_{c,422}$(nm)	$\lambda_{c,424}$(nm)	$\lambda_{c,425}$(nm)	$\lambda_{c,046}$(nm)
1	–	–	–	314.6
2	339.3	339.3	338.6	–
3	379.3	380.6	379.6	–
4	440.8	438.2	437.9	443.7
5	501.1	499.0	499.0	500.7
6	675.0	672.5	674.5	675.3
7	871.4	871.1	869.8	871.5
8	939.8	935.0	937.5	940.2
9	1019.2	1017.9	1019.5	1019.3
10	–	–	1643.4	–

ACPD
12, 4341–4371, 2012

Table 2. Relation of algorithms implemented in the sunrad module in modes 1 and 2.

	mode 1	mode 2
Solar coordinates	Skyrad 4.2.	Blanco-Muriel et al. (2001)
Refraction correction	No	Michalsky et al. (1988)
Optical mass	Single, plane parallel	Multiple; Kasten et al. (1989), Komhyr et al. (1989)
Rayleigh scattering	Fröhlich and Shaw (1980); Young (1981)	Bodhaine et al. (1999)
Ozone absorption	Skyrad 4.2.	Gueymard (2001)
Water vapor absorption	No	Gueymard (2001)
NO_2 absorption	No	Gueymard (2001)
Filter convolution	Gaussian function	Filter transmittance input file
Cloud screening	Smirnov et al. (2001)	Smirnov et al. (2001)
Temperature correction	Compensated (generic coefficients)	Compensated (generic or measured coeff.)
Angström exponents	Ratio of wavelength pairs	Linear regression
Columnar water vapour	Bruegge et al. (1992); Halthore et al. (1997)	Bruegge et al. (1992); Halthore et al. (1997)
Meteo file input	Pressure and ozone	Pressure, ozone, NO_2, water vapor and air temperature

Discussion Paper | Discussion Paper | Discussion Paper | Discussion Paper |
ACPD
12, 4341–4371, 2012
AERONET and ESR sun direct products comparison
V. Estellés et al.

Table 3. Statistics of the differences between ESR-Cimel and AERONET products for mode 1 (top) and mode 2 (bottom). The number of data samples (N) is also indicated. N_{UV} refers to the data available for 340 and 380 channels.

mode 1				N_{UV}=613	N = 933
λ(nm)	rmsd(%)	rmsd	mbd	std	u95
340	11	0.0179	0.0116	0.0137	0.0297
380	5.6	0.0126	0.0041	0.0120	0.0243
440	5.2	0.0109	0.0031	0.0104	0.0211
500	5.7	0.0097	0.0018	0.0095	0.0191
670	7.6	0.0095	0.0037	0.0087	0.0178
870	7.9	0.0084	0.0015	0.0082	0.0165
1020	11	0.0097	−0.0030	0.0092	0.0187
AE	11	0.12	0.02	0.12	0.25
CWV (cm)	9.4	0.17	0.06	0.16	0.33
mode 2					
λ(nm)	rmsd(%)	rmsd	mbd	std	u95
340	2.0	0.0051	0.0007	0.0050	0.0101
380	1.6	0.0036	−0.0021	0.0030	0.0063
440	0.8	0.0016	0.0003	0.0016	0.0033
500	1.0	0.0018	−0.0010	0.0015	0.0031
670	1.3	0.0016	−0.0006	0.0015	0.0031
870	0.5	0.0005	0.0005	0.0002	0.0007
1020	2.2	0.0019	0.0002	0.0018	0.0037
AE	1.4	0.017	−0.007	0.015	0.032
CWV (cm)	7.6	0.147	−0.008	0.146	0.293

ACPD
12, 4341–4371, 2012

Table 4. Statistics of the differences between ESR-Cimel and ESR-Prede products for mode 1 (top) and mode 2 (bottom). The number of data samples (N) is also indicated.

mode 1					$N = 550$
λ(nm)	rmsd(%)	rmsd	mbd	std	u95
440	2.0	0.0038	−0.0023	0.0030	0.0064
500	1.5	0.0025	0.0001	0.0025	0.0050
670	2.1	0.0022	−0.0001	0.0022	0.0045
870	3.0	0.0026	0.0003	0.0026	0.0052
1020	5.3	0.0042	−0.0013	0.0040	0.0080
AE	6.8	0.0772	−0.0495	0.0592	0.1284
CWV (cm)	2.7	0.0520	0.0288	0.0433	0.0913
mode 2					
λ(nm)	rmsd(%)	rmsd	mbd	std	u95
440	1.8	0.0034	−0.0013	0.0032	0.0065
500	3.6	0.0057	0.0044	0.0037	0.0085
670	2.1	0.0023	0.0002	0.0023	0.0046
870	3.0	0.0026	0.0004	0.0026	0.0051
1020	5.7	0.0041	−0.0006	0.0041	0.0082
AE	4.5	0.0537	−0.0091	0.0530	0.1063
CWV (cm)	2.8	0.0528	0.0279	0.0449	0.0940

ACPD
12, 4341–4371, 2012

AERONET and ESR sun direct products comparison

V. Estellés et al.

Table 5. Statistics of the differences between ESR-Prede and AERONET products for mode 1 (top) and mode 2 (bottom). The number of data samples (N) is also indicated.

mode 1					$N = 550$
λ(nm)	rmsd(%)	rmsd	mbd	std	u95
440	5.5	0.0103	−0.0006	0.0103	0.0205
500	5.8	0.0094	0.0005	0.0094	0.0188
670	8.0	0.0089	0.0014	0.0088	0.0176
870	9.3	0.0085	0.0004	0.0085	0.0171
1020	14	0.0117	−0.0057	0.0102	0.0212
AE	12	0.1496	0.0016	0.1496	0.2992
CWV (cm)	10	0.2009	0.1068	0.1701	0.3567
mode 2					
λ(nm)	rmsd(%)	rmsd	mbd	std	u95
440	2.11	0.0039	−0.0007	0.0038	0.0077
500	3.43	0.0054	0.0035	0.0042	0.0090
670	2.46	0.0027	−0.0011	0.0024	0.0050
870	3.18	0.0027	0.0010	0.0026	0.0052
1020	5.70	0.0042	−0.0005	0.0042	0.0083
AE	4.85	0.0570	−0.0153	0.0549	0.1110
CWV (cm)	10.01	0.1953	0.0849	0.1759	0.3619

Discussion Paper | Discussion Paper | Discussion Paper | Discussion Paper |

ACPD

12, 4341–4371, 2012

AERONET and ESR sun direct products comparison

V. Estellés et al.

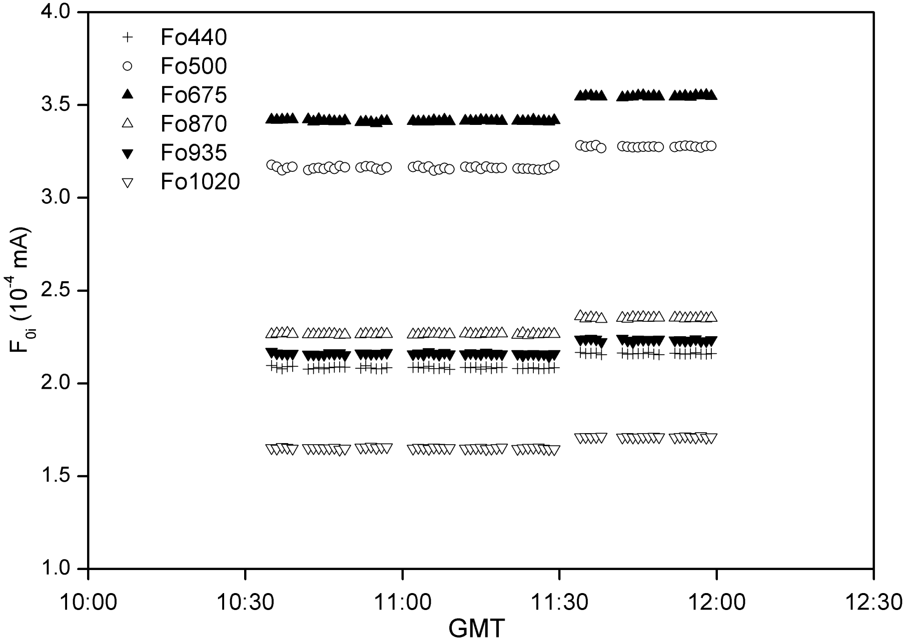

Fig. 1. Calibration transfer example performed on 15 May 2011.

ACPD
12, 4341–4371, 2012

AERONET and ESR sun direct products comparison

V. Estellés et al.

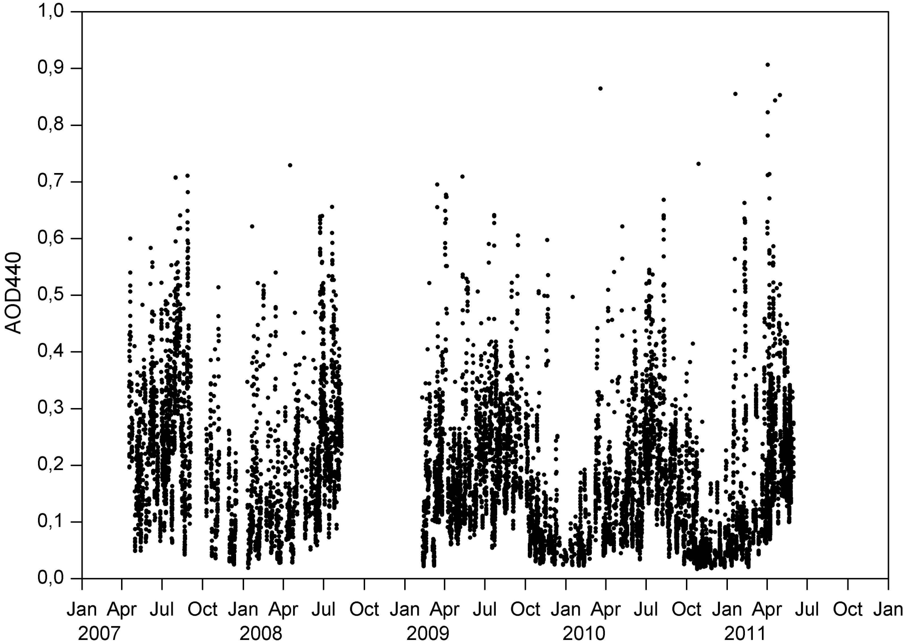

Fig. 2. Evolution of AOD at 440 nm during the period of study.

ACPD
12, 4341–4371, 2012

AERONET and ESR sun direct products comparison

V. Estellés et al.

Title Page
Abstract Introduction
Conclusions References
Tables Figures
Back Close
Full Screen / Esc
Printer-friendly Version
Interactive Discussion

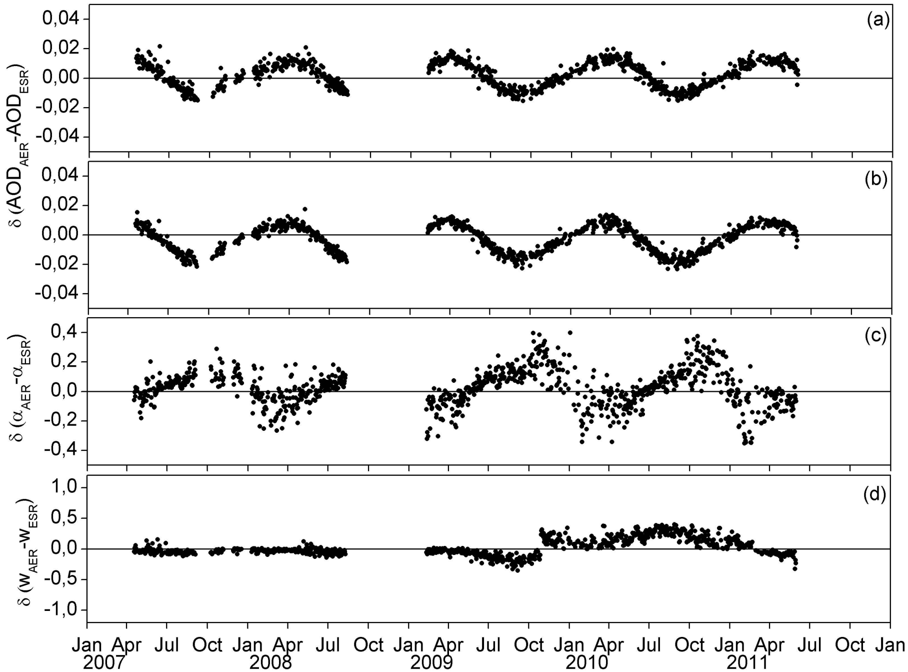

Fig. 3. Evolution of daily averaged differences between ESR-Cimel (mode 1) and AERONET products: **(a)** AOD at 675 nm, **(b)** AOD at 1020 nm, **(c)** Angström exponent, and **(d)** columnar water content.

ACPD
12, 4341–4371, 2012

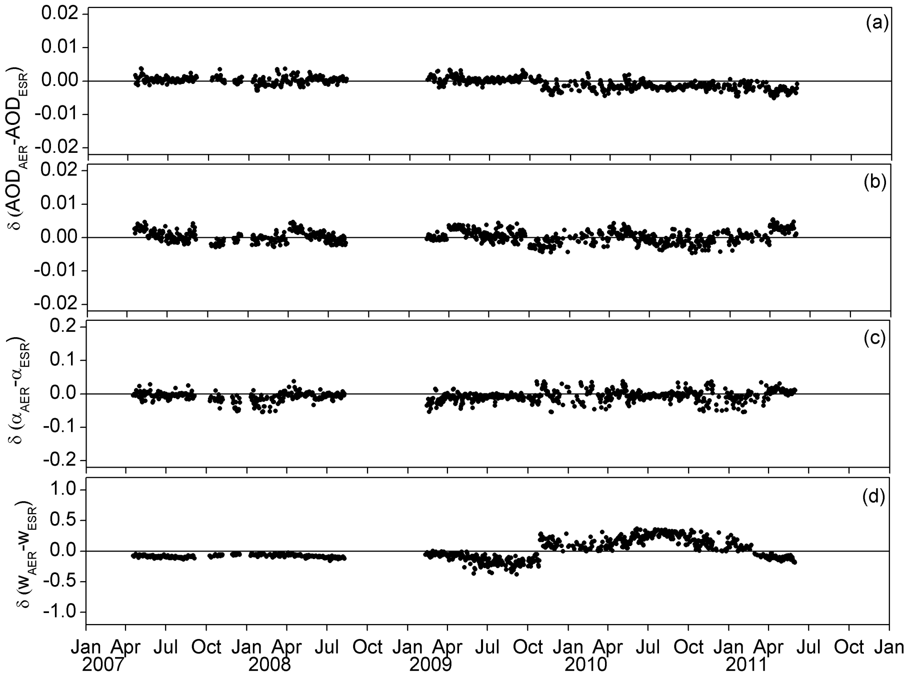

Fig. 4. Evolution of daily averaged differences between ESR-Cimel (mode 2) and AERONET products: **(a)** AOD at 675 nm, **(b)** AOD at 1020 nm, **(c)** Angström exponent, and **(d)** columnar water content.